Iraqi Journal of Veterinary Sciences

www.vetmedmosul.com

Evaluating the toxic oral doses of iron oxide nanoparticles in mice

N.S. Al-Hamadany[1] and M.H. Alzubaidy[2]

[1]Samarra Drug Company, Nineveh Drug Factory, [2]Department of Physiology, Biochemistry and Pharmacology, College of Veterinary Medicine, University of Mosul, Mosul, Iraq

Article information

Article history:
Received February 2023
Accepted May 2023
Available online September 3, 2023

Keywords:
α-Fe2O3-NP
Neurobehavioral
Acute toxicity
Mice

Correspondence:
M.H. Alzubaidy
munaalzubaidy77@yahoo.com

Abstract

Iron nanoparticles (α-Fe_2O_3) are used in a wide range of biological and medicinal applications, including the delivery of specific drugs, other pharmaceutical and agricultural ones. Its toxic effects, risk assessment and safety are still being researched. Hence, in this investigation, 28-day repeated doses for assessing the acute and sub-acute oral toxicity were conducted on (α-$Fe_2O_3$20-40) nanoparticles with special reference to target histopathologically, the neurobehavioral and alteration in mice brain and liver. The acute LD_{50} was 14.74 g/kg orally, using Dixon's method, as well as recording the toxicity signs, such as lethargy, rapid respiration, subcutaneous hemorrhage, plioerection, tremor, and itching. Oral repeated doses for 28 days of α-Fe_2O_3 nanoparticles (75 and 150 mg/kg) led significantly to decrease head pocking, considerable lengthening of negative geotaxis performance, and to a significant decline in open-field activity, compared to the control group. α-Fe_2O_3 nanoparticles at dose 300mg/kg orally in the 7th and 14 days of treatment led to significantly increase mice body weight compared to the control group. The nanoparticles α-Fe_2O_3 at dose 75, 150 and 300mg/kg after 28 days of treatment cause in liver vacuolar degeneration of hepatocytes, congestion of sinusoids, central vein, and necrosis, while in brain, it causes necrosis, gliosis, congestion of blood vessels, thrombus formation and neuronophagia. We conclude that the higher doses and longer exposure to nanoparticles α-Fe_2O_3 show significant toxicity effects represented by neurobehavioral and histopathological changes.

DOI: 10.33899/ijvs.2023.138368.2796,

Introduction

Recent years have witnessed great interest in the use of iron oxide nanoparticles (Fe_2O_3-NPs) in therapeutic and diagnostic applications in CNS (1). There is a lot of research on Fe_2O_3-NPs and their conjugates are used as magnetic resonance imaging (MRI) contrast agents (2). Possessing unique magnetic and paramagnetic properties, as well as their ability to cross the blood-brain barrier, α-Fe_2O_3-NPs are a promising neuroimaging (BBB) platform (3). For assessing CNS tumor lesions, reading, differential diagnosis, image-guided delivery in brain tumor treatment, detecting disease progression, monitoring therapies, and designing specialized treatment plans for CNS disorders (4-7). There is a lot of misinformation regarding the neurotoxic effects of α-Fe_2O_3-NPs on the CNS and their interference with neurobehavioral processes among these high-extending biomedical applications. Based on exposure to various NP concentrations, research in the last ten years has demonstrated the bioaccumulation of NPs and their detrimental consequences in important organs (8). Concerns regarding the biotoxicity of Fe_2O_3-NPs grow as their frequency of biological exposure grows. Fe_2O_3-NPs' clinical effects have been studied and determined to be safe; nevertheless, their molecular interactions with organ systems with repeated and prolonged use need to be examined (9). Since iron is a transition metal, it can easily go through the Fenton's reaction and control the oxidative stress that causes

many neurodegenerative conditions in the brain (10). Despite the critical function of iron in healthy brain physiology and neural development, excessive buildup causes nervous system degeneration (11). In addition, it has been suggested that iron buildup may have a role in the initial stages of neurological memory problems like Alzheimer's disease (12). According to studies by authors (13-16), iron build up in the brain has been linked to oxidative stress, memory loss, impaired motor performance, and neurobehavioral dysfunction. The majority of neurodegenerative illnesses are characterized by a sequence of molecular processes, such as iron buildup, oxidative stress damage, and neuronal death, along with clinical signs such as impaired locomotion and memory loss (17). Exposure to Fe_2O_3-NPs has been shown to cause oxidative stress in the brain, which causes neuronal degeneration (18,19). Significant brain damage is brought on by elevated Fe_2O_3-NP accumulation in the basal ganglia of neuroferritinopathy patients (20). But, clarification of the effects of accumulating Fe_2O_3-NP buildup in the brain and locomotor is needed. It is necessary to lessen the neurotoxic effects of α-Fe_2O_3-NPs due to their high reactivity and the sensitivity of brain tissues to oxidative stress.

The aim of this research is to assess the toxic effects and processes that occur after α-Fe_2O_3- NP buildup in mice model brain system. This investigation looked at how α-Fe_2O_3-NPs affected brain and liver histology, and locomotor behavior.

Materials and methods

Ethical approve

All methods employed in investigations involving animals were upheld to the highest ethical standards by the facility or practice, where the tests were carried out UM.VET 2022.036.

Mice husbandry

We use 74 white male and female mice with body weights ranging from 25 to 35 g, ages between 60 and 90 days, housing them in an animal house.

Preparation of α-Fe_2O_3

Weights of nanoparticles supermagnetic α-Fe_2O_3 98%, 20-40 nm produced by the American company, which were mixed and 10 ml per kilogram of distilled water is used to dissolve it, using ultrasonic cleaner at 20 Hz for 5 minutes at 4ºC to facilitate the dispersion of particles with water (21).

Determination of the acute oral LD_{50} of α-Fe_2O_3-NPs based on the Dixon method

The first dose of α-Fe_2O_3-NPs was set at 10 g/kg for the nine mice that were employed (pilot study). One mouse was kidnapped and given a dose of 10 g/kg; the outcome (the mouse's survival or death) was then determined 24 hours after the dose. After the first change occurs, the dose of three mice individually was administered, taking into account the change in the dose up or down (22-25). The change in the dose amount must occur before the change in the outcome (the mouse's survival or its death) appears.

The effect of oral administering α-Fe_2O_3-NPs at different doses of the median LD_{50} on acute toxicity events in mice

Five groups, each of five mice were created from a total of 25 animals. 10 ml/kg of distilled water was administered to the control group. The second group: the mice were dosed with nanoparticles α-Fe_2O_3 at a dose of 3.69 g/kg, which represents 25% of the LD_{50}. The third group: the mice were dosed with nanoparticles α-Fe_2O_3 at a dose of 7.37 g/kg, which represents 50% of the LD_{50}. The fourth group: the mice were dosed with nanoparticlesα- α-Fe_2O_3 at a dose of 11.06 g/kg, which represents 75% of the LD_{50}. The fifth group: the mice were dosed with nanoparticles α-Fe_2O_3 at a dose of 14.74 g/kg, which represents 100% of the LD_{50}. The mice received therapy, and they were observed for two hours after that, signs of intoxication were recorded, and the toxicity marks were calculated (26).

Sub-acute effects of repeated doses of nanoparticles α-Fe_2O_3

40 mice were divided into four groups randomly, each with 10 mice. For 28 days, the first group (the control group) received doses of distilled water at a rate of 10 ml per kilogram. In the second group, mice received 75 mg/kg of α-Fe_2O_3 nanoparticles. The third group received 150 mg/kg of α-Fe_2O_3 nanoparticles. The fourth group received 300 mg/kg of α-Fe_2O_3 nanoparticles. On the 7^{th}, 14^{th}, and 28^{th} days of dosing.

Open field activity test

To pass this test, you had to count how many squares mice crossed and how many times mice stood on back legs in three minutes (27,28).

Negative geotaxis test

This test shows neuromuscular balance and vestibular function in mice, and the negative geotropism test is performed using a rough wooden surface inclined at an angle of 45 degrees (29), as the head of the mouse is placed longitudinally down the wooden plank, and then according to the time required to rotate the mouse with its entire body 180 degrees toward the top of the inclined surface, and each rat is given a maximum of 60 seconds to turn completely (29).

Pocking head test

This test shows the extent of curiosity and movement of the treated mouse. This test was conducted using a circular plastic surface with a diameter of 30 cm with a small edge with a height of 10 cm containing 8 circular holes with a

diameter of each hole 2 cm. The measurement begins by placing the mouse in the center of the perforated circular surface, then the number of times it enters it is calculated. Mouse head into the holes for 3 minutes (30).

Body weight

The weights of the mice were recorded on the 7th, 14th and 28th days of dosing.

Histopathology

Animals exposed to α-Fe_2O_3 30 were examined histopathological for the liver and brain in both control and treatment groups. Tissues were fixed in 10% neutral buffered formalin following sacrifice. After being embedded in paraffin blocks, the tissues were cut into sections with a microtome. Hematoxylin and eosin and the slide were used to stain 5 µm thick paraffin sections, the slides were examined with microscope at 400X (31,32).

Statistic evaluation

One-way ANOVA was used to examine the data. Its significance was assessed using the least significant test. The Fisher test was used to analyze the frequency data. Non-parametric data were evaluated using the Man Whitney test with a significance level of $P \leq 0.05$ (33).

Results

Determination of the acute oral LD_{50} of nanoparticles α-Fe_2O_3 based on the Dixon method

The oral LD_{50} of nanoparticles α-Fe_2O_3 was 14.74 g/kg, after administering various doses and the appearance of poisoning symptoms represented by lethargy, piloerection, rapid breathing, tremor, hypothermia, subcutaneous hemorrhage, and death (Table 1).

Table 1: The acute oral LD_{50} of nanoparticles α-Fe_2O_3 in mice

Measurements	Results
LD_{50} α-fe_2o_3 nanoparticles	14.74 g/kg
Amounts range	10-15 = 5 g/kg weight
Initial dose	10 g/kg
Final dose	14g/kg
Rising and falling dose	1 g/kg
Number of mice	OOOOOXOXO (9)
Symptoms of poisoning	Rapid breathing, piloerection, tremor, hypothermia, subcutaneous hemorrhage, and death

O: Mouse alive for the past 24 hours. X: Mouse dead for the past 24 hours.

The effect of oral administering of nanoparticles α-Fe_2O_3 at different dose of LD_{50} on acute toxicity

The administration of nanoparticles α-Fe_2O_3 in doses of 25, 50, 75, and 100% which are 3.68,7.37, 11.06, and 14.74 mg/kg, respectively, led to the appearance of the symptoms of toxicity in mice ranging from 20% to 100%, and the signs included lethargy, stillness of movement, rapid breathing, hypothermia, flatulence, tremor, piloerection, itching, subcutaneous hemorrhage, and the toxicity scores were 13, 17, 26, and 25, respectively (Table 2).

Sub-acute effects of repeated doses of nanoparticles α-Fe_2O_3

After 7 days of treatment, oral administration of nanoparticles α-Fe_2O_3 at a dose of 75 mg/kg caused behavioral changes as evidenced by a significant increase in head pocking at doses of 75 and 150 mg/kg and a significant decline in open field activity (rearing and squares crossed) when compared to the control group, respectively (Table 3).

Table 2: Acute toxicity symptom elicited by nanoparticles α-Fe_2O_3 at different dose of LD_{50} on acute toxicity

Parameters	mean ± SE (5 mice /group)			
	Control	3.68 g/kg	7.37g/kg	11.06g/kg
Rapid breathing %	0	80*	80*	100*
Lethargy and motion stillness %	0	0	100*	60
Hypothermia %	0	40	60	100*
Plioerection %	0	40	40	60
Tremor %	0	0	40	60
Subcutaneous hemorrhage %	0	0	0	20
Flatulence%	0	0	0	60
Itching %	0	0	0	20
Grooming %	0	60	40	100*
Score toxicity	0	11	17	26

* Significant change from the control group at $P<0.05$.

Table 3: Neurobehavioral measurements in mice treated with α-Fe_2O_3 Nanoparticles during 7 days of treatment

Variables	Control	Treatment groups with α-Fe_2O_3 at different doses		
		75 mg/kg	150 mg/kg	300 mg/kg
Squares crossed / 3 min	107.20±7.25	76.00±3.00*	116±15.47	119±7.37
Rearing / 3 min	21.20±1.98	13.60±2.52*	19.40±1.29	15.80±2.13
Negative geotaxis (seconds)	11.6±1.60	16.6±3.74	15.8±2.27	11.4±1.54
Head pocking 3 / min	23.60±3.46	34.20±3.81*	33.00±1.92	42.80±3.71*

Values expressed as mean ± SE for 5 mice in each group. *Indicates significant change from the distilled water group at P<0.05.

The behavioral defect was caused by the oral administration of nanoparticles α-Fe_2O_3 at a dose of 300 mg/kg after 14 days of dosing, as evidenced by a significant increase in open field activity (squares crossed and raising) compared to the control group, a significant decrease in the time spent for the negative geotaxis test compared to the control group, and other behavioral changes (Table 4).

After 28 days of treatment, the oral administration of nanoparticles α-Fe_2O_3 at doses of 75 and 150 mg/kg resulted in behavioral defect as shown by a significant decline in open field activity (crossing squares and raising them) compared to the control group, a significant increase in the time spent performing negatively on geotaxis, and a significant decline in head pocking at dose 75 mg/kg, compared to the control group (Table 5).

Sub-acute effects of repeated doses of nanoparticles α-Fe_2O_3 on the body weight

In mice, oral treatment with nanoparticles α-Fe_2O_3 at a concentration of 150,300 mg/kg body weight resulted in a notable rise in body weight on 7, 14 and 28 days (Table 6).

Table 4: Neurobehavioral measurements in mice treated with α-Fe_2O_3 Nanoparticles during 14 days of treatment

Variables	Control	Treatment groups with α-Fe_2O_3 at different doses		
		75 mg/kg	150 mg/kg	300 mg/kg
Squares crossed / 3 min	74.40±3.34	76.80±8.02	91.40±8.05b	106.00±4.55*a
Rearing / 3 min	6.40±0.87	13.60±1.54*	17.60±2.73*	19.20±2.20*
Negative geotaxis (seconds)	14.60±2.25	14.80±2.33	18.00±2.63b	7.80±1.11*a
Head pocking 3 / min	22.40±2.98	16.60±1.89	23.60±2.16	18.00±1.26

Values expressed as mean ± SE for 5 mice in each group. *Indicates significant change from the distilled water group at P<0.05. a indicate significant change from α-Fe_2O_3 treatment at P<0.05.

Table 5: Neurobehavioral measurements in mice treated with α-Fe_2O_3 Nanoparticles during 28 days of treatment

Variables	Control	Treatment groups with α-Fe_2O_3 at different doses		
		75 mg/kg	150 mg/kg	300 mg/kg
Squares crossed / 3 min	81.80±18.39	23.40±2.38*	29.20±5.69*	56.80±5.62
Rearing / 3 min	22.60±2.38	4.80±1.39*	4.20±2.08*	8.40±1.50*
Negative geotaxis (seconds)	5.80±0.73	12.40±1.80*	18.00±1.95*	16.40±2.27*
Head pocking 3 / min	16.00±1.30	8.40±1.50*	19.20±1.88	13.80±2.39

Values expressed as mean ± SE for 5 mice in each group. *Indicates significant change from the distilled water group at P<0.05. a indicate significant change from α-Fe_2O_3 treatment at P<0.05.

Table 6: The effect of repeated doses of α-Fe_2O_3 nanoparticles on the weights of mice for 7, 14 and 28 days

Groups	Weight (grams)		
	7 days	14 days	28 days
Control group	26.80±1.20	25.80±2.08	27.60±2.29
75 mg/kg	28.80±0.37	26.40±1.16	26.40±1.69
150 mg/kg	30.00±0.63*	28.00±0.63	29.20±1.02
300 mg/kg	31.00±1.00*	32.80±1.32*	32.40±2.38

Values expressed as mean ± SE for 5 mice in each group. *Indicates significant change from the distilled water group at P<0.05.

Liver histopathological

The control group showed none of histopathological lesions (Figure 1). The oral administration of nanoparticles α-Fe_2O_3 at dose75mg/kg, caused histopathological defects after 7 days of the dosing, which is evidence by a mild vacuolar degeneration of hepatocytes, sinusoidal dilatation, mild vacuolar degeneration of hepatocytes, central vein congestion, sinusoidal dilatation (Figure 2). While the dose 150mg/kg causes vacuolar degeneration of hepatocytes, infiltration of inflammatory cells, central vein congestion, vacuolar degeneration of hepatocytes, central vein congestion (Figure 3). The dose 300 mg/kg causes mild cell swelling of hepatocytes, congestion of sinusoids, increase number of kupffer cells (Figure 4). Histological section of liver of 75mg/ kg after 14 days of treatment, mild vacuolar degeneration of hepatocytes, congestion of central vein, infiltration of inflammatory cells and increase in number of kupffer cells (Figure 5). While the dose 150 mg/kg after 14 days of treatment causes cell swelling of hepatocytes, congestion of sinusoids, and vacuolar degeneration (Figure 6). The dose 300 mg/kg after 14 days of treatment causes necrosis of hepatocytes, congestion of sinusoids and central vein, vacuolar degeneration, and increase in number of kupffer cells (Figure 7). In 28 days of treatment with nanoparticles α-Fe_2O_3 at dose75mg/kg causes sever vacuolar degeneration of hepatocytes, congestion of sinusoids and central vein, and necrosis (Figure 8). The dose 150 mg/kg after 28 days of treatment with the moderate vacuolar degeneration of hepatocytes, congestion of sinusoids and central vein, necrosis (Figure 9). The dose 300 mg/kg causes sinusoid dilatation (Figure 10).

Brain histopathological

The control group showed none of histopathological lesions (Figure 11). The oral administration of nanoparticles α-Fe_2O_3 at dose75mg/kg, causes histopathological defects after 7 days of the dosing, which is revised by a cortex with perivascular edema, vacuolization and satellitosis (Figure 12). The doses 150 and 300 mg/kg cause vacuolization, cytogenetic edema and neuronophagia (Figures 13 and 14). In 14 days of treatment with nanoparticles α-Fe_2O_3 at dose75, 150 and 300 mg/kg led to cortex with perivascular edema, vacuolization, gliosis, thrombus formation, cytogenetic edema, and satellitosis (Figures 15-17). The nanoparticles α-Fe_2O_3 at dose75,150 and 300 mg/kg after 28 days of treatment, which causes necrosis, gliosis, congestion of blood vessels, thrombus formation and neuronophagia (Figures 18-20).

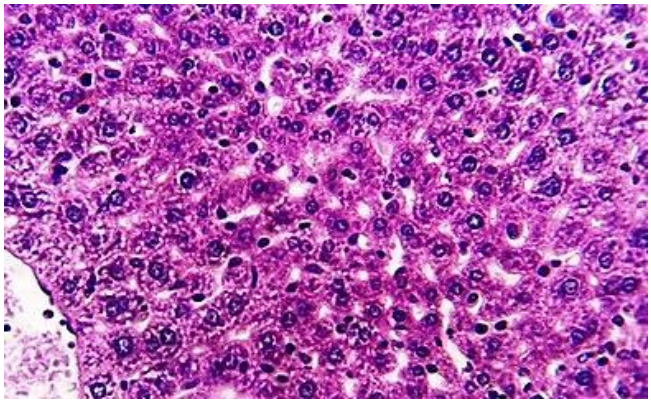

Figure 1: The normal liver architectures are shown in the liver of mice (control group): (a) the central vein, (b) the hepatocytes, and (arrow) the sinusoids. 100x (H&E stain).

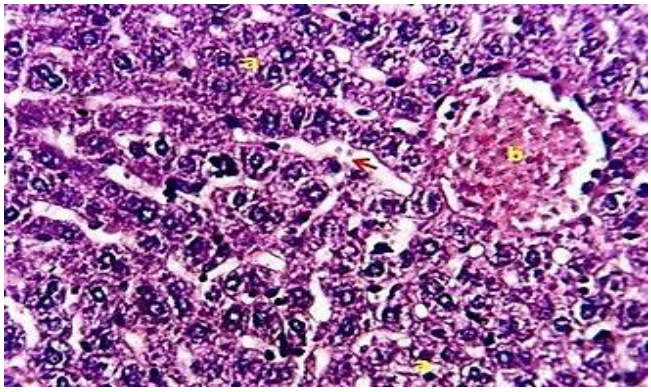

Figure 2: liver of mice dosing75mg /mg for 7days show (a) mild vacuolar degeneration of hepatocytes, (b) central vein congested, (arrow) sinusoidal dilatation. 400x (H&E stain).

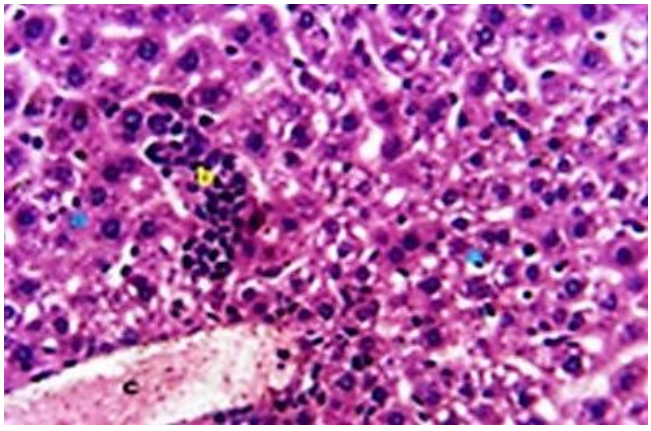

Figure 3 liver of mice 150mg /mg dosing for 7days show (a) vacuolar degeneration of hepatocytes, (b) infiltration of inflammatory cells, (c) central vein congestion. 400x (H&E stain).

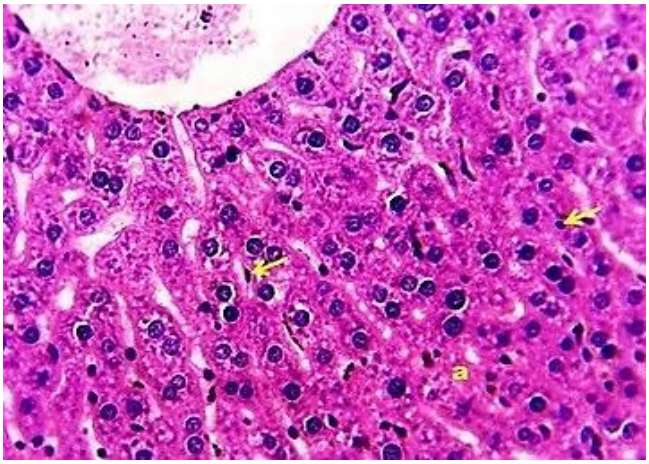

Figure 4: liver of mice dosing 300mg/mg for 7days show (a) mild cell swelling of hepatocytes, (arrow) increase number of Kupffer cells. 400x (H&E stain).

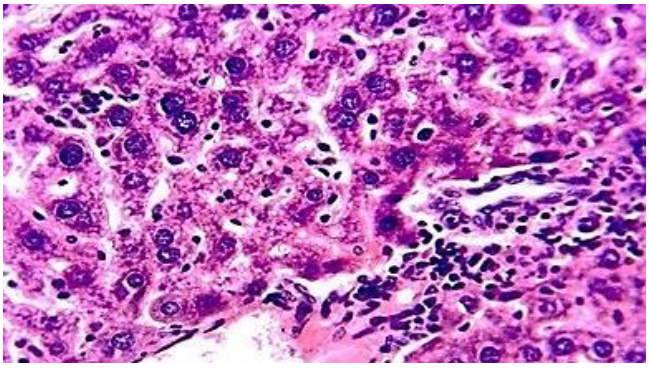

Figure 5: liver of mice dosing 75mg / kg for 14 days show (a) mild vacuolar degeneration of hepatocytes, (arrow) central vein congested, (c) infiltration of inflammatory cells, (arrow) increase number of kupffer cells. 400x (H&E stain).

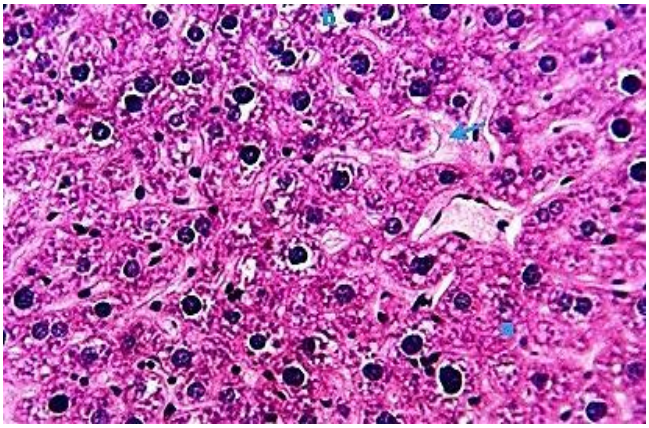

Figure 6: liver of mice dosing 150mg/kg for 14 days show (a) cell swelling of hepatocytes, (arrow) sinusoids congested, and (b) vacuolar degeneration. 400x (H&E stain).

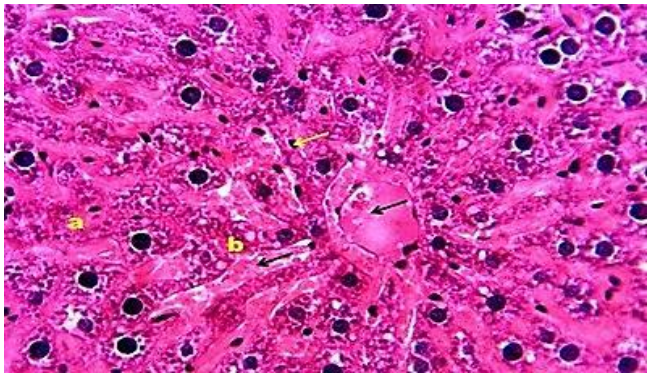

Figure 7: liver of mice dosing 300mg / kg for 14 days show (a) necrosis of hepatocytes, (black arrow) sinusoids congested and central vein, and (b) vacuolar degeneration, (yellow arrow) increase number of Kupffer cells. 400x (H&E stain).

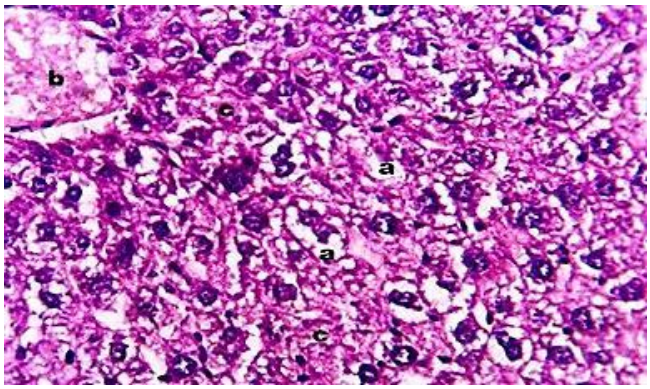

Figure 8: liver of mice dosing 75mg/kg for 28 days show (a) sever vacuolar degeneration of hepatocytes, (b) sinusoids congested and central vein, (c) necrosis. 400x (H&E stain).

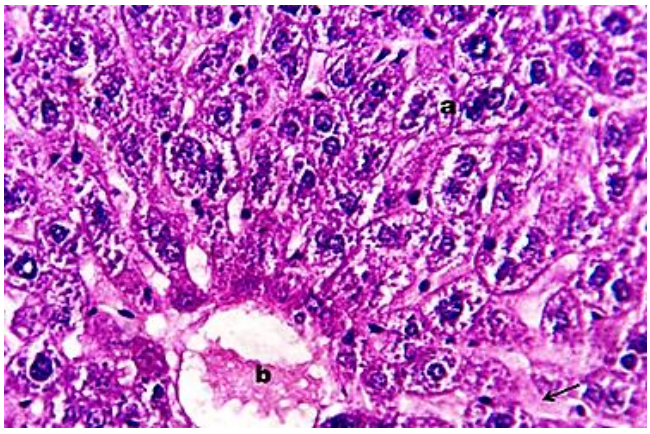

Figure 9: liver of mice dosing150mg/kg for 28 days show (a) moderate vacuolar degeneration of hepatocytes, (b) sinusoids congested and central vein, (c) necrosis. 400x (H&E stain).

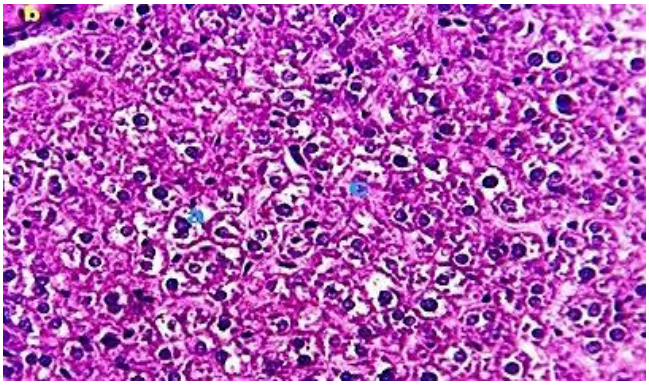

Figure 10: liver of mice dosing 150mg/kg for 28 days show (a) mild vacuolar degeneration of hepatocytes, (b) sinusoids congested and central vein, and (arrow) sinusoid dilatation. 400x (H&E stain).

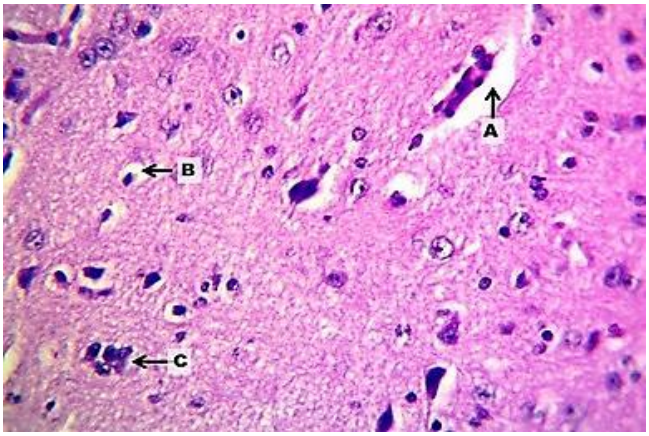

Figure 11: The normal brain mice showing normal architecture representing by neurons (A), glial cells (B) and blood vessels (C). 400x (H&E stain).

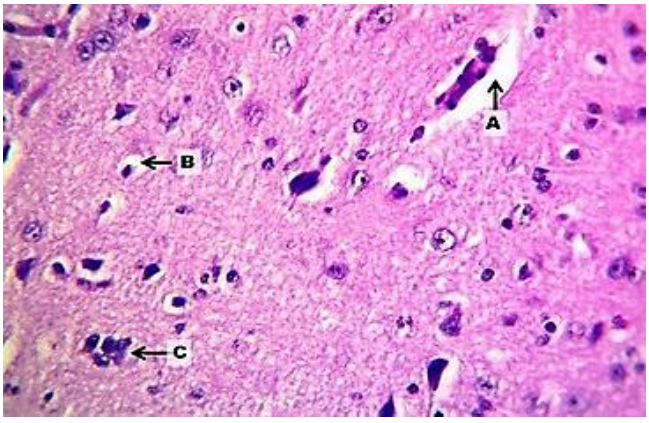

Figure 12: Brain of mice dosing 75 mg/kg for 7 days showing the cortex with perivascular edema (A), vacuolization (B) and satellitosis (C). 400x (H&E stain).

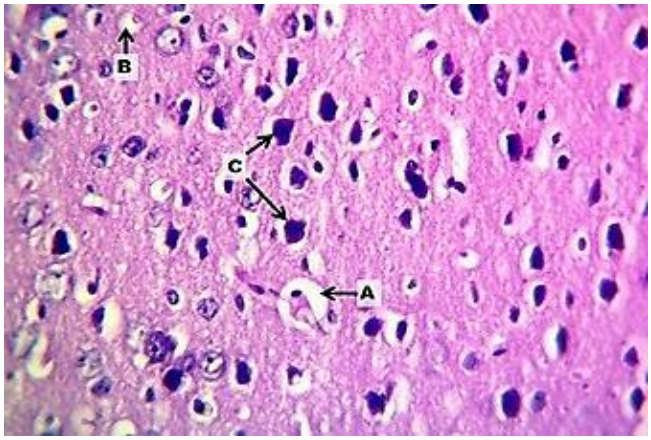

Figure 13: Brain of mice dosing 150 mg /kg for 7 days showing the cortex with perivascular edema (A), vacuolization (B) and cytogenetic edema (C). 400x (H&E stain).

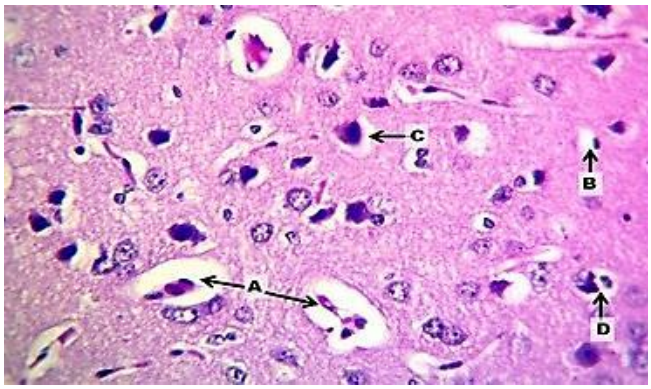

Figure 14: Brain of mice dosing 300 mg/kg for 7 days showing the cortex with perivascular edema (A), vacuolization (B), cytogenetic edema (C) and neuronophagia (D). 400x (H&E stain).

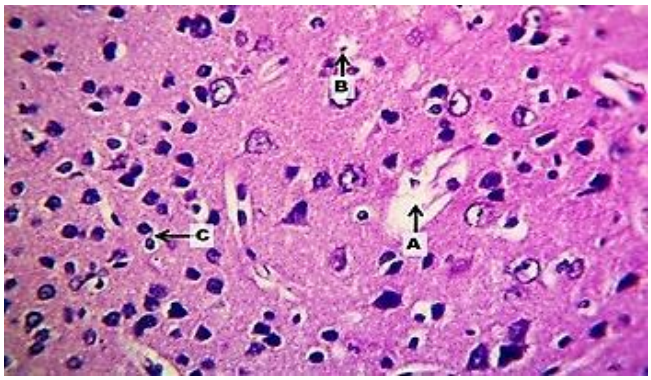

Figure 15: Brain of mice dosing 75 mg /kg for 14 days showing the cortex with perivascular edema (A), vacuolization (B) and gliosis (C). 400x (H&E stain).

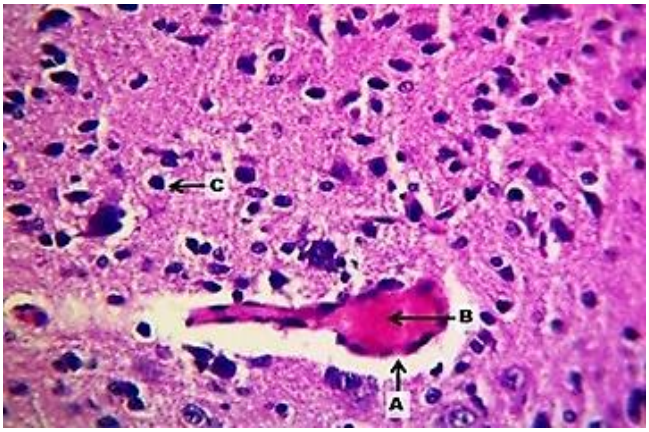

Figure 16: Brain of mice dosing 150 mg/kg for 14 days showing the cortex with perivascular edema (A), thrombus formation (B) and cytogenetic edema(C). 400x (H&E stain).

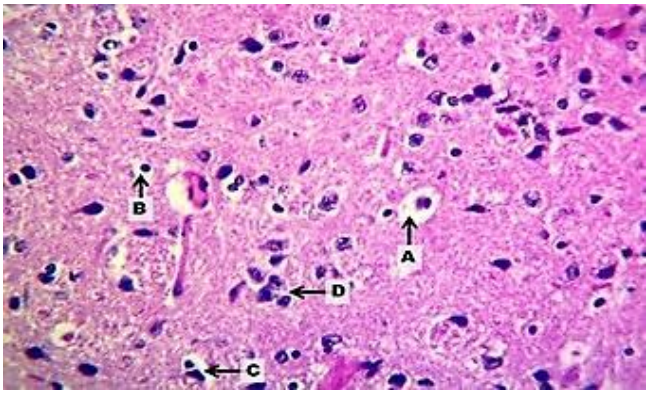

Figure 17: Brain of mice dosing 300 mg/kg for 14 days showing the cortex with perivascular edema (A), vacuolization (B), cytogenetic edema (C) and satellitosis (D). 400x (H&E stain).

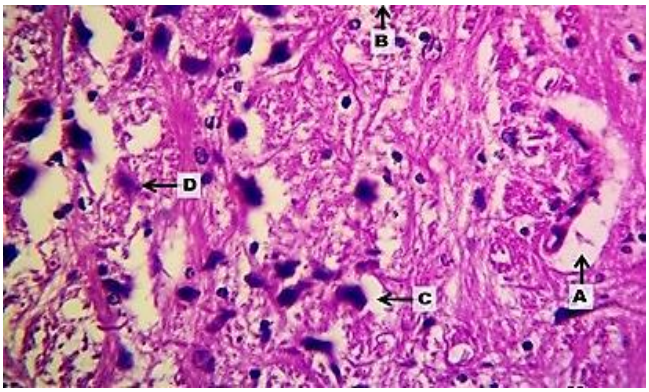

Figure 18: Brain of mice dosing 75 mg/kg for 28 days showing the cortex with perivascular edema (A), vacuolization (B), cytogenetic edema (C) and necrosis (D). 400x (H&E stain).

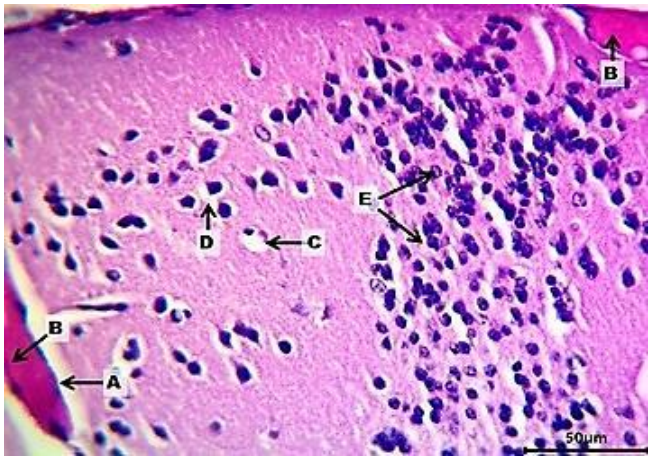

Figure 19: Brain of mice dosing 150 mg/kg for 28 days showing the cortex with perivascular edema (A), congestion of blood vessels (B), vacuolization (C), cytogenetic edema (D) and gliosis (E). 400x (H&E stain).

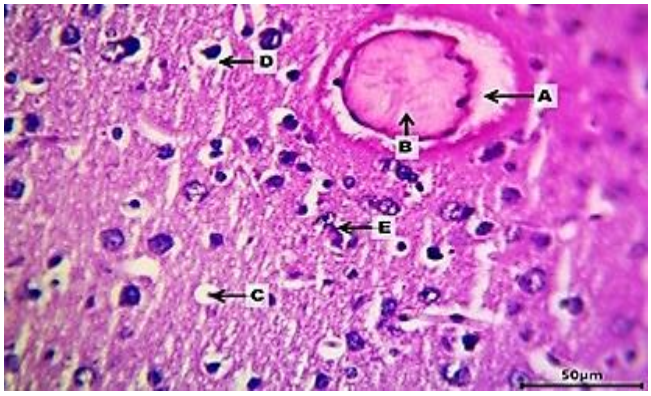

Figure 20: Brain of mice dosing 300 mg for 28 days showing the cortex with perivascular edema (A), thrombus formation (B), vacuolization (C), cytogenetic edema (D) and neuronophagia (E). 400x (H&E stain).

Discussion

Due to the limited information about the acute toxic effect of α-Fe_2O_3 nanoparticles in mice, the current study focused on determining the LD_{50} of α-Fe_2O_3 nanoparticles for the first time and recording signs and scores of poisonings as well as its effects on the neurobehavioral and histological sections of the liver and brain of mice.

In general, α-Fe_2O_3- NPs are thought to be secure, biocompatible, and non-poisoning substances. This is proven by our results by determining the acute oral LD_{50} in mice, which was 14.7 g/kg, while the available data of uncoated iron oxide nanoparticles' LD_{50} was estimated to be between 300 and 600 mg/kg (34). This number was increased to 2000-6000 mg/kg when the iron oxide nanoparticles were coated

with stabilizing and biocompatible dextran molecules (34). This is based on how compounds are classified using the Globally Harmonized Classification System (GHS) that belongs to the unclassified toxicity, which means that α-Fe_2O_3 nanoparticles is rather safe in mice (35).

The highest toxic doses of α-Fe_2O_3 nanoparticles in mice causes symptoms of acute toxicity, such as lethargy, rapid respiration, subcutaneous hemorrhage, plioerection, tremor, flatulence, and itching. While the clinical toxic symptoms following acute oral administration in rat is dullness, irritation, and moribund signs (36). In humans, the toxic signs are nausea, vomiting, and flatulence (37). Also, they include headache, urticarial, pruritus, and back pain, chest pain, dyspnea, a skin rash, a drop in oxygen saturation, and anaphylactic shock (38).

The current work focuses on the numerous behavioral changes including the head pocking test (30), which reveals the negative effects on the brain and its cognitive function, the negative geotaxis test (29), which increases the duration of negative geotaxis performance due to a defect in the vestibular system, and the open-field activity test (28), which lowers motor activity due to central nervous system inhibition caused by repeated exposure to α-Fe_2O_3-nanoparticals for 28 days. Since Fe_2O_3-nanoparticals buildup has been proven to have negative effects on the CNS and aggravate neurodegenerative illnesses (18,19), much research is being done to shed light on the safety concerns of Fe_2O_3-nanoparticals exposure. According to De Lima *et al.* (16) and Budni *et al.* (39), oxidative stress mechanisms and apoptosis are linked to behavioral alterations (40). By producing free radicals, Fe_2O_3-nanoparticals cause oxidative stress and collapse the antioxidant defense system. The animals exposed to α-Fe_2O_3-nanoparticles repeatedly experience their entrance and buildup in the CNS due to BBB damage. Accumulated α-Fe_2O_3-nanoparticals interact with the important biomolecules, negatively affecting neuronal physiology and opening the door to alterations in behavior (41).

Similar to Kumari *et al.* and Manseel *et al.* (36,42) test groups subjected to low, medium, and high doses of α-Fe_2O_3 nanoparticles repeatedly till 28 days showed no reduction in body weight in the exposed mice. Wang *et al.* (43) reported considerable weight loss, gastro-intestinal damage, and severe discomfort in contrast to these observed results.

A considerable amount of microscopic damage was seen in all major organs (liver and brain) during a histopathological evaluation of the harvested tissues. Fe binding proteins such as transferrin and ferritin, which act as carriers of Fe to various tissues, appear to have an influence on the observed differential organ distribution pattern of Fe_2O_3 nanoparticles in a dose dependent. Wang *et al.* (44) also discovered accumulation of Fe_2O_3 nanoparticles at an oral dose of 600 mg/kg in the major organ systems of mice, supporting the aforementioned findings. Numerous reports have examined the poisoning of Fe_2O_3 nanoparticles (45,46). However, there is a discrepancy between the stated results. According to Kim *et al.* (47) Fe_2O_3 nanoparticles do not appear to be hazardous to mice. However, numerous other studies (48-50) have documented serious deleterious consequences linked to exposure to these Fe_2O_3 nanoparticles (47). In the current investigation, the majority of the organs, including the liver, exhibited histological alterations that were mostly caused by vascular congestion. Even when the α-Fe_2O_3 nanoparticles are tailored for tissue or organ specific targeting (e.g., tumors), liver is expected to contain the most efficient nanoparticle clearance system, which accounts for the observed vascular alterations in the highest dosage group (36,42).

Conclusion

The study findings suggest that mice exposure to α-Fe_2O_3 nanoparticles can cause neurodegeneration and behavioral abnormalities. It is discovered that the toxicity of α-Fe_2O_3 nanoparticles increases with concentration. As a result, it is possible to draw the further conclusion that doses and the duration of exposure to - α-Fe_2O_3 nanoparticles cause unfavorable histological alterations that could harm cellular functions. Given the quick development of α-Fe_2O_3-NP applications, the findings call for an understanding that is essential, not only for safety considerations, but also for their repeated biomedical applications in the future.

Acknowledgement

Sincere thanks are due to Department of Physiology, Biochemistry, and Pharmacology, and to College of Veterinary Medicine, University of Mosul.

Conflict of interests

The writers declare that they have no interests in opposition.

References

1. Prina-Mello A, Crosbie-Staunton K, Salas G, Morales MP, Volkov Y. Multiparametric toxicity evaluation of SPIONs by high content screening technique: Identification of biocompatible multifunctional nanoparticles for nanomedicine. IEEE Trans Magn. 2013;49(1):377-382. DOI: 10.1109/TMAG.2012.2225024
2. McCullough B, Kolokythas O, Maki J, Green D. Ferumoxytol in clinical practice: Implications for MRI. J Magn Reson Imaging. 2012;36:1476-1479. DOI: 10.1002/jmri.23879
3. Winer J, Kim P, Law M, Liu C, Apuzzo M. Visualizing the future: Enhancing neuroimaging with nanotechnology. WLD Neurosurg. 2011;75:626-637. DOI: 10.1016/j.wneu.2011.02.016
4. Varallyay CG, Nesbit E, Fu R, Gahramanov S, Moloney B, Earl E, Muldoon LL, Li X, Rooney WD, Neuwelt EA. Highresolution steady-state cerebral blood volume maps in patients with central nervous system neoplasms using ferumoxytol, a superparamagnetic iron oxide nanoparticle. J Cereb Blood Flow Metab. 2013;33:780-786. DOI: 10.1038/jcbfm.2013.36

5. Fan CH, Ting CY, Lin HJ, Wang CH, Liu HL, Yen TC, Yeh CK. SPIO-conjugated, doxorubicin-loaded microbubbles for concurrent MRI and focused-ultrasound enhanced brain-tumor drug delivery. Biomater. 2013;34:3706-3715. DOI: 10.1016/j.biomaterials.2013.01.099
6. Wadghiri Y, Li J, Wang J, Hoang D, Sun Y, Xu H, Tsui W, Li Y, Boutajangout A, Wang A, de Leon M, Wisniewski T. Detection of amyloid plaques targeted by bifunctional USPIO in Alzheimer's disease transgenic mice using magnetic resonance microimaging. PLOS One. 2013;8:57097. DOI: 10.1371/journal.pone.0057097
7. Frechou M, Beray-Berthat V, Raynaud JS, Meriaux S, Gombert F, Lancelot E, Plotkine M, Marchand-Leroux C, Ballet S, Robert P, Louin G, Margaill I. Detection of vascular cell adhesion molecule-1 expression with USPIO enhanced molecular MRI in a mouse model of cerebral ischemia. Contrast Media Mol Imaging. 2013;8:157-164. DOI: 10.1002/cmmi.1512
8. Chen Z, Meng H, Xing G, Chen C, Zhao Y, Jia G, Wang T, Yuan H, Ye C, Zhao F, Chai Z, Zhu C, Fang X, Ma B, Wan L. Acute toxicological effects of copper nanoparticles in vivo. Toxicol Lett. 2006;163:109-120. DOI: 10.1016/j.toxlet.2005.10.003
9. Winer JL, Liu CY, Apuzzo ML. The use of nanoparticles as contrast media in neuroimaging: A statement on toxicity. WLD Neurosurg. 2012;78:709-711. DOI: 10.1016/j.wneu.2011.08.013
10. Halliwell B. Oxygen radicals as key mediators in neurological disease: Fact or fiction. Ann Neurol. 1992;32:10-15. DOI: 10.1002/ana.410320704
11. Schipper HM. Neurodegeneration with brain iron accumulation clinical syndromes and neuroimaging. Biochim Biophys Acta Mol Basis Dis. 2012;1822:350-360. DOI: 10.1016/j.bbadis.2011.06.016
12. Thompson KJ, Shoham S, Connor JR. Iron and neurodegenerative disorders. Brain Res Bull. 2011;55:155-164. DOI: 10.1016/s0361-9230(01)00510-x
13. Fredriksson A, Schroder N, Eriksson P, Izquierdo I, Archer T. Neonatal iron exposure induces neurobehavioural dysfunctions in adult mice. Toxicol Appl Pharmacol. 1999;159:25-30. DOI: 10.1006/taap.1999.8711
14. Fredriksson A, Schroder N, Eriksson P, Izquierdo I, Archer T. Maze learning and motor activity deficits in adult mice induced by iron exposure during a critical postnatal period. Brain Res Dev. 2000;119:65-74. DOI: 10.1016/s0165-3806(99)00160-1
15. Schroder N, Fredriksson A, Vianna MR, Roesler R, Izquierdo I, Archer T. Memory deficits in adult rats following postnatal iron administration. Behav Brain Res. 2011;124:77-85. DOI: 10.1016/s0166-4328(01)00236-4
16. De Lima MN, Polydoro M, Laranja DC, Bonatto F, Bromberg E, Moreira JC, Dal-Pizzol F, Schröder N. Recognition memory impairment and brain oxidative stress induced by postnatal iron administration. Eur J Neurosci. 2005;21(9):2521-8. DOI: 10.1111/j.1460-9568.2005.04083.x
17. Ali YO, Escala W, Ruan K, Zhai RG. Assaying locomotor, learning, and memory deficits in drosophila models of neurodegeneration. J Vis Exp. 2011;11(49):2504. DOI: 10.3791/2504
18. Wang B, Feng WY, Wang M, Shi JW, Zhang F, Ouyang H, Zhao YL, Chai ZF, Huang YY, Xie YN, Wang HF, Wang J. Transport of intranasally instilled fine α-Fe_2O_3 particles into the brain: Micro-distribution, chemical states, and histopathological observation. Biol Trace Elem Res. 2007;118:233-243. DOI: 10.1007/s12011-007-0028-6
19. Wang B, Feng W, Zhu M, Wang Y, Wang M, Gu Y, Ouyang H, Wang H, Li M, Zhao Y, Chai Z, Wang H. Neurotoxicity of low-dose repeatedly intranasal instillation of nano- and submicron-sized ferric oxide particles in mice. J Nano Res. 2009;11:41-53. DOI: 10.1007/s11051-008-9452-6
20. Hautot D, Pankhurst QA, Morris CM, Curtis A, Burn J, Dobson J. Preliminary observation of elevated levels of nanocrystalline iron oxide in the basal ganglia of neuroferritinopathy patients. Biochim Biophys Acta. 2007;1772(1):21-25. DOI: 10.1016/j.bbadis.2006.09.011
21. Dhakshinamoorthy V, Manickam V, Perumal E. Neurobehavioural toxicity of iron oxide nanoparticles in mice. Neurotox Res. 2017;32:187-203. DOI: 10.1007/s12640-017-9721-1
22. Dixon WJ. Efficient analysis of experimental observations. Annu Rev Pharmacol Toxicol. 1980;20:441-462. DOI: 10.1146/annurev.pa.20.040180.002301
23. Naser AS, Albadrany YM. The neurobehavioral effects of flumazenil in chicks. Iraqi J Vet Sci. 2021;35(4):783-788. DOI: 10.33899/ijvs.2020.128443.1577
24. Al-Zubaidy MI, Mustafa KH, Al-Baggou BH. Neurobehavioral and biochemical toxicity of atrazine in chicks. Vet Ir Zootech. 2022;80(1):51-56. [available at]
25. Al-Zubaidy MI, Amin SM, Alsangary DH. Neurotoxicity of xylazine in chicks. Iraqi J Vet Sci. 2023;37(1):289-296. DOI: 10.33899/ijvs.2022.135299.2463
26. Alrawe SA, Al-Zubaidy MI. Acute and sub-acute toxicity effects of lambda-cyhalothrin in chicks. Iraqi J Vet Sci. 2022;36(1):191-200. DOI: 10.33899/ijvs.2021.129674.1678
27. Al-Najmawi TH, Al-Zubaidy MI. Acute toxicity events of ivermectin in chicks, model. Iraqi J Vet Sci. 2022;36(4):1119-1124. DOI: 10.33899/ijvs.2022.133188.2188
28. Molinengo L, Fundarò A, Orsetti M. The effect of chronic atropine administration on mouse motility and on Ach levels in the central nervous system. Pharmacol Biochem Behav. 1989;32(4):1075-1077. DOI: 10.1016/0091-3057(89)90085-3
29. Mohammad FK, St VO. Behavioral and developmental effects in rats following in utero exposure to 2, 4-D/2, 4, 5-t mixture. Neurotoxicol Teratol. 1986;8(5):551-560. DOI: 10.1016/j.ntt.2011.09.006
30. Soni K, Parle M. Anxiolytic effects of *Trachyspermum ammi* seeds in mice. J Pharm Sci Pharmacol. 2017;3(1):71-4. DOI: 10.1166/jpsp.2017.1077
31. Jaber MT, Al-Jumaa ZM, Al-Taee SK, Nahi HH, Al-Hamdany MO, Al-Salh MA, Al-Mayahi B. Bioaccumulation of heavy metals and histopathological changes in muscles of common carp (*Cyprinus Carpio L.*) in the Iraqi rivers. Iraqi J Vet Sci. 2021;35(2):245-249. DOI: 10.33899/ijvs.2020.126748.1368
32. Al-Zubaidy MI. Acute neurotoxicity of acetaminophen in chicks. Vet Arh. 2021;91(4):379-387. DOI: 10.24099/vet.arhiv.0950
33. Katz M. Study design and statistical analysis: A practical guide for clinicians. UK: Cambridge University Press; 2006. 66-119 p.
34. Wada S, Yue L, Tazawa K, Furuta I, Nagae H, Takemori S, Inamimura T. New local hyperthermia using dextran magnetite complex (DM) for oral cavity: experimental study in normal hamster tongue. Oral Dis. 2001;7:192-195. DOI: 10.1034/j.1601-0825.2001.70309.x
35. Grodzki K. Establishing a globally harmonised hazard classification and labelling system for dangerous substances and preparations. Tutb News. 2000;14:17-23. DOI: 10.1016/s0378-4274(01)00529-x
36. Kumari M, Rajak S, Singh SP, Kumari SI, Kumar PU, Murty US, Mahboob M, Grover P, Rahman MF. Repeated oral dose toxicity of iron oxide nanoparticles: Biochemical and histopathological alterations in different tissues of rats. J Nanosci Nanotechnol. 2012;12(3):2149-2159. DOI: 10.1166/jnn.2012.5796
37. Masselli G, Gualdi G. MR imaging of the small bowel. Radiol. 2012;264:333-348. DOI: 10.1148/radiol.12111658
38. Bernd H, De Kerviler E, Gaillard S, Bonnemain B. Safety and tolerability of ultrasmall superparamagnetic iron oxide contrast agent: Comprehensive analysis of a clinical development program. Invest Radiol. 2009;44(6):336-342. DOI: 10.1097/RLI.0b013e3181a0068b
39. Budni P, de Lima MN, Polydoro M, Moreira JC, Schroder N, Dal-Pizzol F. Antioxidant effects of selegiline in oxidative stress induced by iron neonatal treatment in rats. Neurochem Res. 2007;32:965-972. DOI: 10.1007/s11064-006-9249-x
40. Miwa CP, de Lima MN, Scalco F, Vedana G, Mattos R, Fernandez LL, Hilbig A, Schröder N, Vianna MR. Neonatal iron treatment increases apoptotic markers in hippocampal and cortical areas of adult rats. Neurotox Res. 2011;19:527-535. DOI: 10.1007/s12640-010-9181-3
41. Kovacic P, Somanathan R. Nanoparticles: Toxicity, radicals, electron transfer, and antioxidants. In: Armstrong D, Bharali D, editors. Oxidative stress and nanotechnology methods in molecular biology. Totowa: Humana Press; 2013. 15-35 p.

تقييم التأثير السمي المتناول عن طريق الفم لدقائق أوكسيد الحديد النانوي في الفئران

نشوان عدنان الحمداني[١] و منى حازم إبراهيم الزبيدي[٢]

[١]شركة أدوية سامراء، مصنع أدوية نينوى، [٢]فرع الفسلجة والكيمياء الحياتية والأدوية، كلية الطب البيطري، جامعة الموصل، الموصل، العراق

الخلاصة

تستخدم دقائق أوكسيد الحديد النانوية في العديد من التطبيقات البيولوجية والطبية ومنها توصيل الأدوية. مع ذلك، فان الدراسات حول أثارها السمية على الفئران محدودة. بناء على ذلك، كان الهدف من دراستنا الحالية تقييم السمية الفموية الحادة وتحت الحادة لمدة ٢٨ يوم لدقائق الحديد من خلال دراسة التغييرات السلوكية العصبية والنسيجية للكبد والدماغ. سجلت الجرعة المميتة الوسطية وكانت ١٤,٧٤ غرام /كغم عن طريق الفم باستخدام طريقة ديكسون كما تم تسجيل علامات التسمم مثل الخمول، التنفس السريع، النزيف تحت الجلد، الحكة، انتفاخ البطن، وانتصاب الشعر. أدى إعطاء دقائق الحديد النانوية وبجرع ٧٥ و١٥٠ ملغم /كغم عن طريق الفم ولمدة ٢٨ يوم الى انخفاض كبير في النشاط الحركي داخل الميدان المفتوح رافقه نقصان كبير في عدد مرات إدخال راس الفار في الثقوب وزيادة كبيرة في المدة اللازمة لعودة الفار الى وضعه الطبيعي في اختبار الانتحاء الأرضي السالب مقارنة مع مجموعة السيطرة. كما أدت الجرعة ٣٠٠ ملغم /كغم لمدة ٧ و ١٤ يوم الى زيادة كبيرة في أوزان الفئران مقارنة مع مجموعة السيطرة. وأدى إعطاء دقائق الحديد النانوية وبجرع ٧٥ و١٥٠ و ٣٠٠ ملغم /كغم لمدة ٢٨ يوم الى تغييرات نسيجية في الكبد ومنها تنكس فجوي للخلايا الكبدية واحتقان في الجيبانيات والوريد المركزي فضلاً عن النخر، بينما شملت التغييرات النسيجية في الدماغ النخر والاحتقان في الأوعية الدموية وتكوين الخثرات ووذمة حول الأوعية الدموية والبلع العصبي. نستنتج من دراستنا الحالية أن سمية دقائق أوكسيد الحديد تزداد بزيادة الجرعة وفترة التعرض وأظهرت هذه التأثيرات تغييرات سلوكية عصبية ونسيجية في الفئران.

42. Manseel TH, Niharika S, Smitall K. Sub-acute Toxicity assessment of green synthesized hematite nanoparticles (Fe2O3 NPs) using Wistar rat. Res J Biotechnol. 2020;15(4):121-135. [available at]
43. Wang B, Feng W, Wang M, Wang T, Gu Y, Zhu M, Ouyang H, Shi J, Zhang F, Zhao Y, Chai Z. Acute toxicological impact of nano-and submicro-scaled zinc oxide powder on healthy adult mice. J Nanopart Res. 2008;10(2):263-276. DOI: 10.1007/s11051-007-9245-3
44. Wang Y, Wang B, Zhu MT, Li M, Wang HJ, Wang M, Ouyang H, Chai ZF, Feng WY, Zhao YL. Microglial activation, recruitment and hagocytosis as linked phenomena in ferric oxide nanoparticle exposure. Toxicol Lett. 2011;205(1):26-37. DOI: 10.1016/j.toxlet.2011.05.001
45. Reddy UA, Prabhakar PV, Mahboob M. Biomarkers of oxidative stress for in vivo assessment of toxicological effects of iron oxide nanoparticles. Saudi J Biol Sci. 2017;24(6):1172-1180. DOI: 10.1016/j.sjbs.2015.09.029
46. Sadeghi L, Tanwir F, Babadi VY. In vitro toxicity of iron oxide nanoparticle: Oxidative damages on Hep G2 cells. Exp Toxicol Pathol. 2015;67(2):197-203. DOI: 10.1016/j.etp.2014.11.010
47. Kim WY, Kim J, Park JD, Ryu HY, Yu IJ. Histological study of gender differences in accumulation of silver nanoparticles in kidneys of Fischer 344 rats. J Toxicol Environ Health A. 2009;72(21-22):1279-84. DOI: 10.1080/15287390903212287
48. Starmans LW, Moonen RP, Aussems-Custers E, Daemen MJ, Strijkers GJ, Nicolay K, Grüll H. Evaluation of iron oxide nanoparticle micelles for magnetic particle imaging (MPI) of thrombosis. PLOS One. 2015;10(3):1-15. DOI: 10.1371/journal.pone.0119257
49. Szalay B, Tátrai E, Nyírő G, Vezér T, Dura G. Potential toxic effects of iron oxide nanoparticles in in vivo and in vitro experiments. J Appl Toxicol. 2012;32(6):446-453. DOI: 10.1002/jat.1779
50. Vandhana S, Nithya M, Deepak A. Review on nano toxic effects in living organisms (mice and zebra fish). Int J Innov Res Sci Technol. 2015;1(8):134-137. [available at]